# Tip-induced domain structures and polarization switching in ferroelectric amino acid glycine

E. Seyedhosseini' , I. Bdikin, M. Ivanov, D. Vasileva, A. Kudryavtsev, B. J. Rodriguez, and A. L. Kholkin

Citation: Journal of Applied Physics **118**, 072008 (2015); doi: 10.1063/1.4927807
View online: http://dx.doi.org/10.1063/1.4927807
View Table of Contents: http://aip.scitation.org/toc/jap/118/7
Published by the American Institute of Physics

JOURNAL OF APPLIED PHYSICS **118**, 072008 (2015)

# Tip-induced domain structures and polarization switching in ferroelectric amino acid glycine

E. Seyedhosseini,[1,a)] I. Bdikin,[2] M. Ivanov,[1] D. Vasileva,[3] A. Kudryavtsev,[4] B. J. Rodriguez,[5] and A. L. Kholkin[1,3]
[1]*CICECO Aveiro Institute of Materials and Department of Physics, University of Aveiro, 3810 193 Aveiro, Portugal*
[2]*TEMA and Department of Mechanical Engineering, University of Aveiro, 3810 193 Aveiro, Portugal*
[3]*Institute of Natural Sciences, Ural Federal University, 620000 Ekaterinburg, Russia*
[4]*Moscow State Institute of Radioengineering, Electronics and Automation, 119454 Moscow, Russia*
[5]*Conway Institute of Biomolecular and Biomedical Research and School of Physics, University College Dublin, Dublin, Ireland*

(Received 3 December 2014; accepted 24 March 2015; published online 19 August 2015)

Bioorganic ferroelectrics and piezoelectrics are becoming increasingly important in view of their intrinsic compatibility with biological environment and biofunctionality combined with strong piezoelectric effect and a switchable polarization at room temperature. Here, we study tip-induced domain structures and polarization switching in the smallest amino acid $\beta$-glycine, representing a broad class of non-centrosymmetric amino acids. We show that $\beta$-glycine is indeed a room-temperature ferroelectric and polarization can be switched by applying a bias to non-polar cuts via a conducting tip of atomic force microscope (AFM). Dynamics of these in-plane domains is studied as a function of an applied voltage and pulse duration. The domain shape is dictated by polarization screening at the domain boundaries and mediated by growth defects. Thermodynamic theory is applied to explain the domain propagation induced by the AFM tip. Our findings suggest that the properties of $\beta$-glycine are controlled by the charged domain walls which in turn can be manipulated by an external bias. © *2015 AIP Publishing LLC*. [http://dx.doi.org/10.1063/1.4927807]

## I. INTRODUCTION

Inorganic piezoelectric and ferroelectric materials are widely used for temperature and force sensing, data storage, mechanical actuation, and, recently, for energy harvesting.[1] They are based mainly on perovskites (presumably containing lead) and sintered at high temperature thus preventing their integration into Si-based devices and use in biomedical applications. Organic ferroelectric materials,[2] on the contrary, can be easily processed (e.g., by solution growth) and easily functionalized, e.g., for biosensor applications. In addition, they are mechanically flexible and, therefore, can provide conformal coating.[3] However, they typically suffer from low spontaneous polarization, low transition temperature, and weak piezoelectric properties even at low temperatures. Recent results on croconic acid[4] and disopropylammonium chloride (bromide)[5,6] have been indeed a breakthrough due to a combination of high enough transition temperature and polarization combined with low coercive field and switchability. These discoveries paved the way for using organic ferroelectrics in bioelectronics, biosensing, harvesting systems, MEMS, just to name a few. For example, biologically compatible harvesting elements were created based on 1,4-diazabicyclo[2.2.2] octane perrhenate (dabcoHReO$_4$) ferroelectric microcrystals embedded in polymer fibers by electrospinning.[7] However, these materials represent a relatively narrow class of synthetic organic crystals with a limited variability of the physical properties and rarely known biocompatibility. Apparently, new materials classes based on natural tissue components, such as amino acids, peptides, or lipids, should be explored in view of their natural biocompatibility and variability.[8] Recent studies on the simplest amino acid glycine have demonstrated that it is a suitable material with apparent ferroelectric properties and square piezoresponse hysteresis loops at room temperature.[9] The advantage of glycine is not only its simplicity and ability to serve as a building block for proteins but also its polymorphic nature allowing simple yet effective means to form piezoelectric composites comprising several phases of the same material (e.g., ferroelectric-dielectric or ferroelectric-piezoelectric). Recently, a simple method of stabilization of the piezoelectric $\beta$-phase has been demonstrated,[10] and a humidity effect on the motion of the interphase boundary has been revealed.[11] The ability to grow stable $\beta$-phase crystals has allowed us to study in detail its switchability and dynamics of the ferroelectric domain propagation in this technologically important material. The domain shape is dictated by polarization screening at the domain boundaries and also mediated by growth defects. Thermodynamic theory is applied to explain the domain size under switching by the voltage applied to the tip of the atomic force microscope (AFM) and 180° domain wall energy is extracted from the experiments. Our findings suggest that $\beta$-glycine is an uniaxial ferroelectric with the properties controlled by the charged domain walls which in turn can be manipulated by the tip-enhanced electric field.

[a)]Author to whom correspondence should be addressed. Electronic mail: Seyedhosseini@ua.pt

 

## II. EXPERIMENTAL

Needle-shaped $\beta$-glycine crystals were grown via evaporation of a 50 $\mu$l drop of 0.13 M aqueous glycine solution onto (111)Pt/$SiO_2$/Si substrate (Inostek, South Korea) under ambient conditions (21 °C, humidity 30%).[10]

In this work, we used AFM, namely, its piezoresponse force microscopy (PFM) configuration[12] to study local piezoelectricity in $\beta$-glycine micro crystals either by simple polarization imaging or using a spectroscopy mode. In PFM imaging, an ac voltage is applied locally to the sample via PFM tip leading to the sample deformation due to converse piezoelectric effect. It is possible to record both deflection and torsion displacements of the cantilever on the sample surface, thus acquiring vertical (out-of-plane) and lateral (in-plane) piezoresponses. A commercial AFM (Ntegra Aura, NT-MDT, Russia) used in this study was equipped with an external function generator (FG120,Yokogawa, Japan) and a lock-in amplifier (SR830, Stanford Research, USA). A conductive Si cantilever with a spring constant of ~3 N/m and resonance frequency of ~75 kHz (measurement frequency ~15 kHz) was used for domain imaging and local poling. Switching spectroscopy PFM was performed to confirm polarization switchability of domains.[13] In these measurements, the tip was fixed at a predefined position on the sample surface and voltage bias pulses of variable strengths and durations were applied. Domain configurations were imaged immediately after each pulse. In some cases, we could observe an instability of the switched domains (polarization backswitching). In these cases, several scans were done until a more or less stable domain configuration was reached.

## III. RESULTS AND DISCUSSION

Figures 1(a) 1(c) show typical topography and piezoresponse images (separately amplitude and phase) acquired on the surface of a needle-shaped $\beta$-glycine microcrystal comprising several domain boundaries. According to the topography image (Fig. 1(a)), $\beta$-glycine grows in a layer fashion and a number of defects are generated on the surface of the crystal. These topographic defects apparently correlate with the distribution of ferroelectric domains. Only an in-plane (shear piezocontrast) was observed with almost zero out-of-plane polarization (image not shown). The bright and dark contrasts of the in-plane phase image (Fig. 1(c)) indicate an apparent 180° phase difference and suggest an antiparallel polarization direction in adjacent domains (as shown in Fig. 1(c) by arrows). The in-plane (shear) signal is significantly reduced at domain walls as expected (Fig. 1(d)).[14] This could be a result of domain wall clamping and averaging effect of the piezoresponse by the finite size of the tip.[14] A comparison of the in-plane piezoresponse with single crystal x-ray diffraction data (obtained on identical $\beta$-glycine crystals elongated along the *b* direction[10]) indicates that the spontaneous polarization of as-grown domains is *parallel* to the crystal axis *b* of the monoclinic phase of a $\beta$-polymorph. By calibrating lateral displacement using an AFM scanner, it was possible to determine the absolute value of the effective shear piezoelectric coefficient ($d_{15\text{eff}}$) inside the domain. The in-plane sensitivity was calculated based on the geometry of the cantilever and measured out-of-plane deflection sensitivity as described by Peter *et al.*[15] The piezoresponse signal of $\beta$-glycine was measured at a point inside the domain while varying the amplitude of the ac bias from 0 to 15 V.

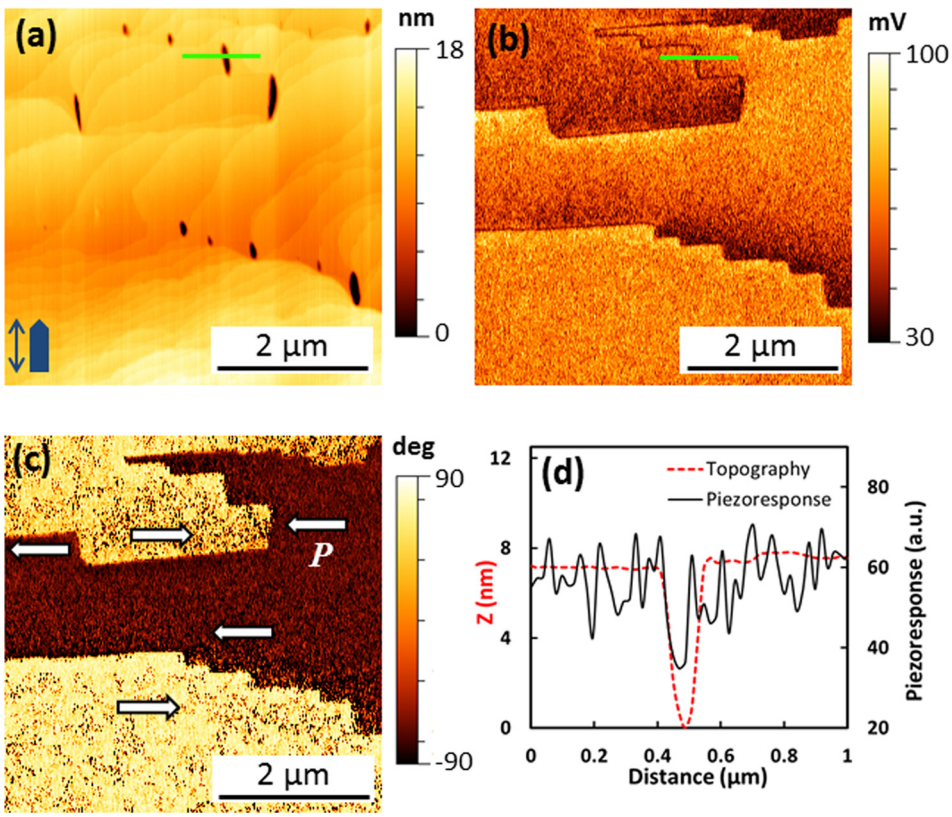


FIG. 1. (a) Topography, (b) LPFM (lateral PFM) amplitude, (c) LPFM phase, and (d) cross sections across the domain wall on the topography and amplitude images (marked by green line).

The effective shear piezoelectric coefficient was calculated directly from the slope of the acquired curve and in-plane torsional sensitivity of the cantilever.[15] The value varied from point to point with an average effective coefficient of about 6 pm/V. It should be noted that this value cannot represent the true bulk coefficient and should be used with caution to evaluate piezoelectric activity of the amino acid crystals. Still this value is significantly greater than that of the corresponding coefficient of quartz ($d_{14} = 0.76$ pm/V)[16] and similar to ZnO ($d_{15} = 8.3$ pm/V).[17]

The domain walls in $\beta$-glycine are apparently true 180° domains separating domains with the polarization parallel to the domain wall plane and charged domain walls in which polarization discontinuity leads to an additional energy associated with such domain configurations. The combination of both represents a typical step-like domain structure similar to that recently observed in α-6,6′-dimethyl-2,2′-bipiridinium chloranilate.[18] Figure 2 shows a part of the step-like domain structure overlaid on the 3D topography image. It clearly indicates that the 180° domains are mostly coincident with the cleavage planes of the crystal. The steps in topography correspond to the atomic planes of $\beta$-glycine. Since the crystal surface was not polished, it may be suggested that the stabilization of 180° domain walls occurs at these growth defects and their density is controlled by the density of atomic steps on the surface. It is natural to propose that $\beta$-glycine (grown at room temperature below the Curie point) could decrease the domain wall energy by pinning 180° domain walls at the vertical steps on the surface (Fig. 2). These thermodynamically stable domains may not be easily switched under an applied electric field and thus the macroscopic remanent polarization can be reduced as compared to the single domain state.[18]

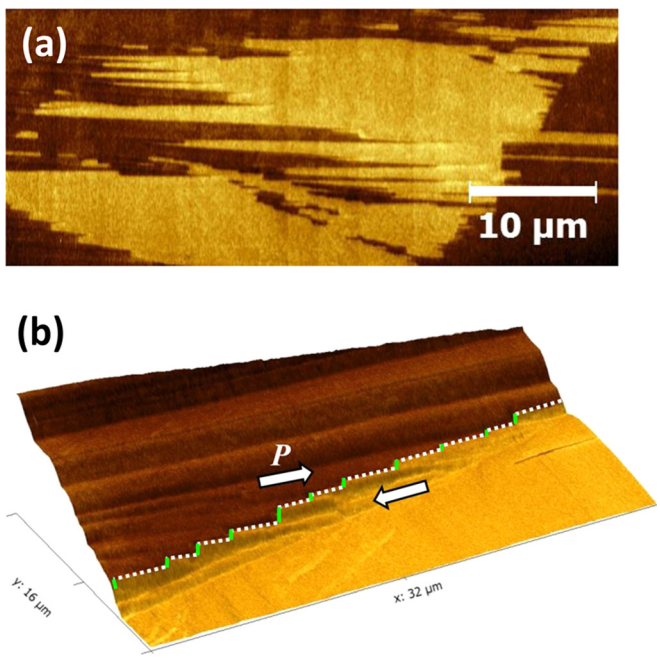


FIG. 2. (a) LPFM contrast for the as grown state, (b) PFM contrast overlaid on the topography. Green and white lines represent charged and neutral do main walls, respectively.

The distinct feature of our $\beta$-glycine microcrystals is a presence of a large number of charged domain walls (either head-to-head or tail-to-tail). In uniaxial ferroelectrics, 180° domain walls typically separate antiparallel domains with polarization vector *parallel* to domain plane, so as to avoid high electrostatic energy associated with polarization discontinuity at the domain wall.[19] Consequently, charged domain walls have been rarely observed in ferroelectric materials, e.g., in $PbTiO_3$ crystals,[20] in PZT thin films[21] and, recently, in uniaxial organic ferroelectrics.[18] An as-grown glycine crystal has both antiparallel (neutral) and charged ferroelectric domain walls appearing as a series of steps as shown schematically in Fig. 3. As seen from the comparison of PFM amplitude and topography cross-sections (Fig. 1(d)), the initial charged domain boundaries in the crystal are always associated with the topography trenches of about 6 7 nm in depth. This is an indication of the existence of topological defects which can be associated with the high electrostatic field compensated by electronic or ionic charges trapped at defect sites.[22] On the other hand, the associated strain at the charge domain wall is about 0.1% and corresponds to the change of crystal dimension due to $d_{31}$ piezoelectric effect under an electric field of about 5 MV/cm. This naturally explains the existence of trenches (not protrusions) on the surface due to the negative sign of $d_{31.}$ Unfortunately, our microcrystals were by far too small to conduct conventional Sawyer-Tower polarization hysteresis measurements.

In order to confirm polarization switchability in $\beta$-glycine, an external electric field was applied locally via a PFM tip to the crystal with in-plane polarization and domain switching was controlled by varying the amplitude and duration of dc bias pulses.[23] It is well known that the electric field created via PFM tip is inhomogeneous and has a maximum intensity in a direction perpendicular to the sample surface. Due to this effect, it is possible to create an artificial domain with the polarization perpendicular to the ferroelectric surface and monitor their switching kinetics by measuring the domain diameter versus applied voltage.[24,25] Recently, Pertsev and Kholkin[26] have theoretically shown that the 180° in-plane polarization switching can be observed in uniaxial ferroelectrics when the initial polarization is *parallel* to the sample surface. In this approach, the PFM tip is represented as a line of charges[25] and the potential distribution created by the tip inside the ferroelectric crystal can be written in the form

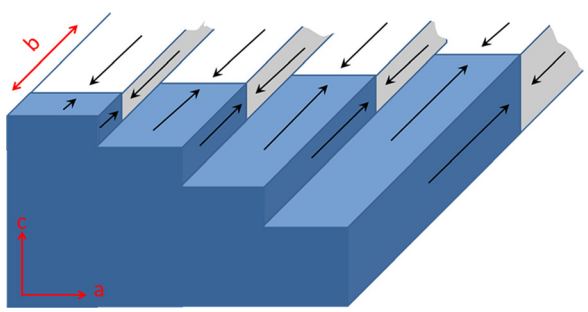


FIG. 3. Schematic of the domain configurations and polarization distribution on the growth steps of glycine crystals.

$$\phi_{tip} = \frac{V}{\ln\left[\frac{2H\sqrt{\varepsilon_x\varepsilon_z}}{(r_{tip}\,\varepsilon_{ext})}\right]} \ln\left[\frac{H - \sqrt{\varepsilon_x/\varepsilon_z}z + \sqrt{x^2 + (\varepsilon_x/\varepsilon_y)y^2 + \left(H - \sqrt{\varepsilon_x/\varepsilon_z}z\right)^2}}{h - \sqrt{\varepsilon_x/\varepsilon_z}z + \sqrt{x^2 + (\varepsilon_x/\varepsilon_y)y^2 + \left(h - \sqrt{\varepsilon_x/\varepsilon_z}z\right)^2}}\right], \quad (1)$$

where $x$ is a coordinate parallel to the polar axis (in our case $b$ direction), $z$ is the coordinate perpendicular to the surface, $H$ is the total tip height, $r_{tip}$ is the effective radius of the tip, $\varepsilon_{ext}$ is the dielectric permittivity of external media, and $V$ is the bias applied to the tip. The dielectric response in the surface plane is supposed to be anisotropic ($\varepsilon_x \neq \varepsilon_y$), where $\varepsilon_x$ is the dielectric permittivity along the polar $x$ direction and $\varepsilon_y$ is along the nonpolar one. The distribution of lateral field of the tip should be calculated as the derivative of potential $\phi_{tip}$ with respect to $x$: $E_x^{tip} = -\partial\phi_{tip}/\partial x$.

We calculated the lateral component of electric field intensity at the sample surface and at two different depths (10 and 20 nm) by using Eq. (1) and applied voltage 90 V. As expected, the inhomogeneous electric field induced by the tip in x-direction ($E_x^{tip}$) has opposite signs at right and left sides from the tip, reaching a maximum at a distance close to the tip and then decreasing slowly with distance (Fig. 4(a)). Therefore, the surface domain would grow only at one side of the PFM tip depending on the initial polarization of the crystal and the sign of applied electric field (Fig. 4(b)). Changing the bias sign reverses the direction of electric field produced by the tip and, therefore, creates a domain in the opposite direction (Fig. 4(c)). Interestingly, recent observation of the in-plane switching in congruent $LiNbO_3$ single crystals demonstrate much richer phenomena where in-plane domains grew in the same direction after the application of voltages of opposite signs.[27]

Indeed, after the application of a high enough dc bias to the tip in contact with the glycine surface, a new 180° domain is observed being sufficiently stable after switching. Figures 5(a) and 5(b) represent domains appearing after the application of −90 V to the tip for two opposite polarization states (cf. Figs. 5(a) and 5(b)) and different pulse durations. The direction of the nascent domain is sensitive to the initial polarization direction and changes to the opposite one upon crystal rotation at 180°. Nascent domains have a typical rectangular shape with high aspect ratio and wedge-shaped end (in order to decrease electrostatic energy associated with charged domain wall[19]). We note that the charged domain walls are not associated anymore with the surface morphology defects (i.e., with the topography change) and, therefore, electrically switched domains were not that stable as compared to the natural ones appearing during crystal growth. It is speculated that the high electrostatic field associated with them could be partly compensated by the external rather than by internal charges associated with defects. It was found that as-grown charged domain walls cannot be moved even under very high electric bias (up to 100 V) applied to the tip.

Domain lengths were found to be dependent on the amplitude and duration of the applied voltage pulses. Figure 6

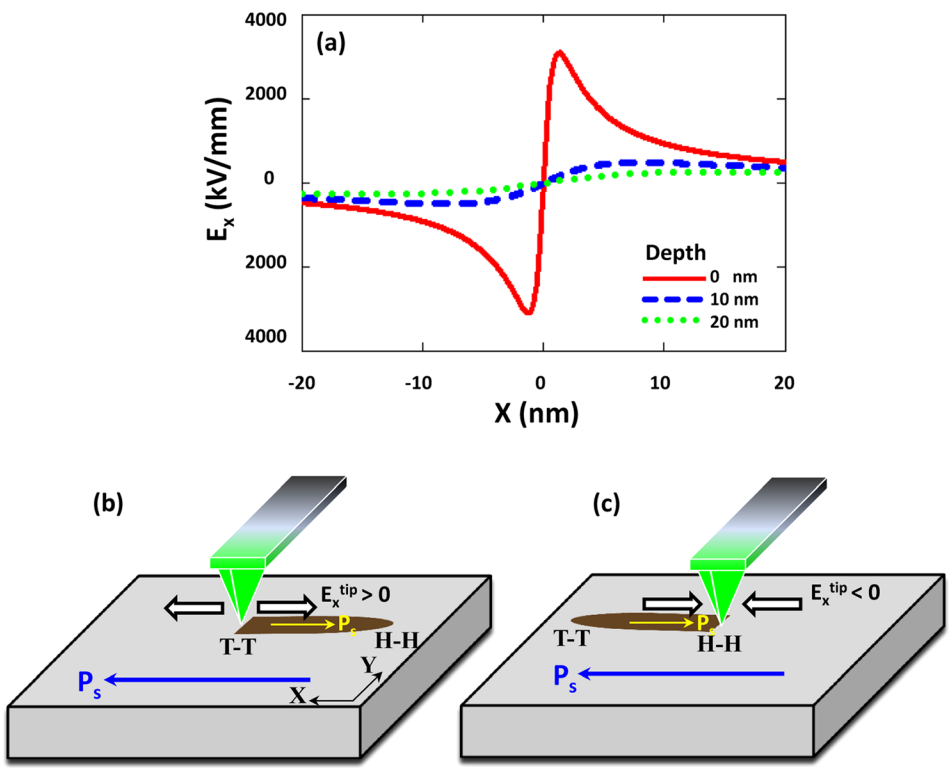


FIG. 4. (a) The electric field intensity $E_x^{tip}$ produced by the tip on the surface and with different depths along the x axis. (b) and (c) Schematics of the expected in plane domain configuration recorded by the PFM tip with positive and negative bias, respectively. T T is tail to tail and H H is head to head configurations.

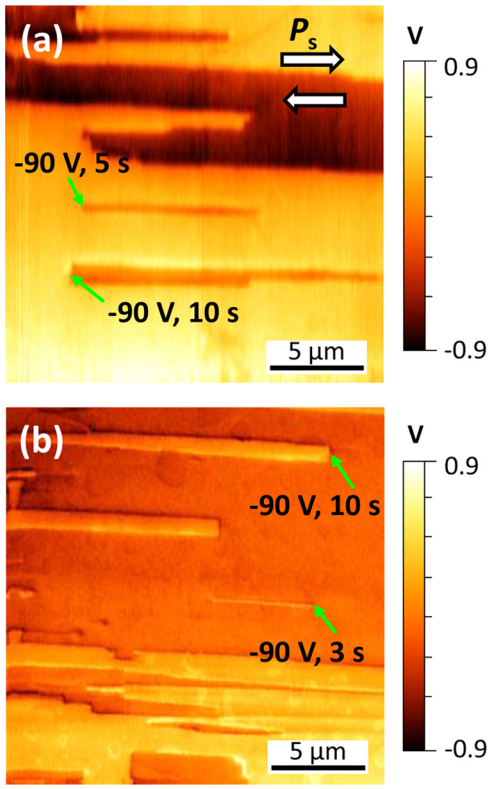


FIG. 5. LPFM image of domains after writing in bright (a) and dark areas (b) by tip voltages of 90 V with different pulse durations (the arrows show the contact points of the AFM tip).

illustrates the voltage dependence of the domain length for a fixed bias pulse duration (10 s). Independently of the voltage pulse duration, the critical voltage was about 65 V for both orientations of the initial polarization. Small variation of critical voltages (±5 V) probably originates from different defect structure (density, defect type) under the tip.

The value of threshold voltage needed for the appearance of domains on the non-polar surface is more than three times higher than that necessary for the switching on the polar surface in glycine ($V_{cr} \approx 20\,V$ according to Ref. 9). There are two reasons for that. First, due to the dielectric anisotropy of the surface $(\varepsilon_z/\varepsilon_x > 2)$, the maximum value of $E_z$ is about two times higher than that of $E_x$, similar to the case of the non-polar surface of uniaxial $LiNbO_3$.[27] Second, back switching effect could be more pronounced for in-plane domains which are not sufficiently stable due to incomplete polarization screening.[27] Apparently, domains switched under lower voltages are unstable, and the initial polarization state is recovered after the external field is switched off. This happens due to fundamental instability of the charged domain which cannot be completely screened with absence of the slow bulk screening processes.[28]

Ferroelectricity in organic crystals arises from the collective transfer of electrons in charge-transfer (CT) complexes[29] or protons transfer in hydrogen bonded crystals,[2] which are different from ionic displacements in perovskite structure. The spontaneous polarization of glycine crystals come from the interaction of permanent dipole moments of glycine molecules in the volume but polarization of each chain can be inverted by dynamics of the intermolecular N-H…O bonds, similar to proton tautomerism of O-H…O bonds in croconic acid[30] or N-H…N bonds in benzimidazole derivatives.[31] This property is attributed to the amphoteric nature of glycine molecule which can donate or accept proton to each other.

With increasing voltage, the domain length reached high values, e.g., ∼17 $\mu$m for 90 V, or even more as shown in Fig. 6. At such distances, the associated driving field from the tip is very weak or practically zero (according to $E_x^{tip}$ equation). Thus the domain wall is not driven anymore by the electric field from the tip. This observation can be explained by the domain breakdown phenomenon, a domain

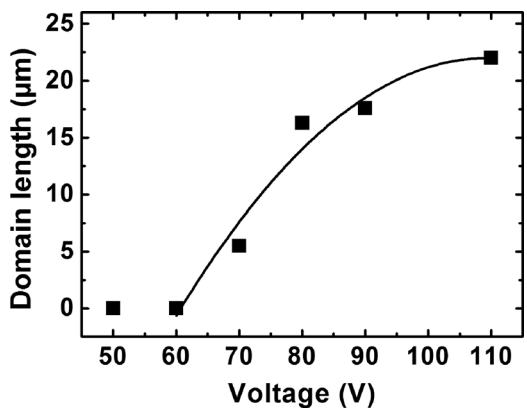


FIG. 6. Domain length as a function of applied voltage for a fixed pulse duration (10 s).

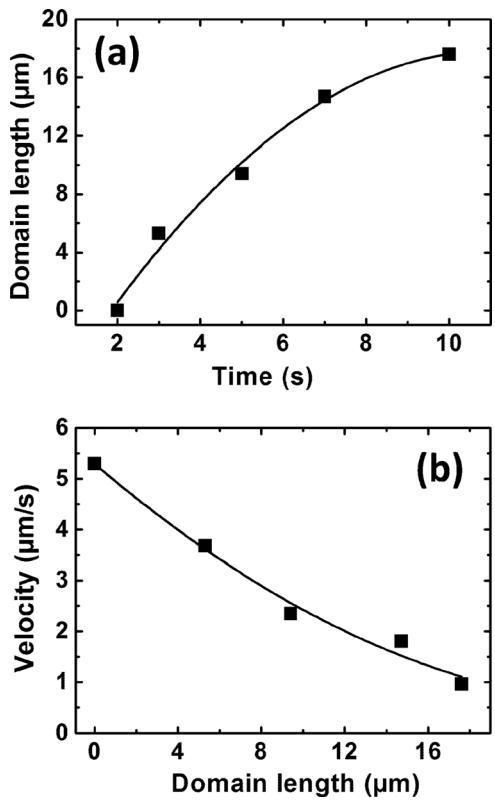


FIG. 7. (a) Domain length as a function of writing time for the applied voltage 90 V. (b) Domain wall velocity of as a function of domain length for the applied voltage 90 V.

growth process which was proposed by Molotskii *et al.*[32] It states that the main driving force for domain propagation is a decrease in the depolarizing field energy of the system, rather than direct effect of the electric field induced by the tip. Probably, in the case of glycine, the domain length increases with consecutive rear-rangement of H atoms position in the intermolecular N-H…O bonds to satisfy the minimum free energy condition.

The domain lengths were also found to depend on the duration of the applied voltage as seen in Fig. 7(a). The threshold time was about 2 s. At shorter times, the domains were not in equilibrium and switched back after the field was removed. Domain wall velocity was calculated based on the dependence of the domain length on switching time ($\nu = dL/dt$) and is plotted as a function of the domain length in Fig. 7(b). Domain velocity significantly decreases with increasing domain length since the lateral electric field asymptotically decreases with distance from the tip ($E_x^{tip} \sim 1/x$).[26]

The stability of the written domain structures is important for the application of ferroelectrics for memories and other applications.[33] In glycine, the domains are stable for a short time only and then their length slowly decreases to reach stable configuration or sometimes they fully disappear similar to the case of single-domain strontium-barium niobate (SBN) crystals.[34] However, the time taken for the nucleated domain to switch back after removal of the field is much slower than the intrinsic switching time.

The equilibrium domain size under the voltages above the critical one was determined using a theoretical approach developed in Ref. 26, and the results were compared with the experimental results in Fig. 6. The model is based on the minimization of the total free energy after the polarization switching inside the domain in the form $\Delta F = U_{dw} + U_{dep} - 2P_s \int_\Omega E_x^{tip}(x,y,z)d\Omega$, where $U_{dw}$ is the self-energy of the domain boundary separating the new domain from the surrounding crystal, $U_{\text{dep}}$ is the energy of a depolarizing field created by the polarization charges on the domain surface, and the last term represents the work $W_{\text{tip}}$ done by $E_{\text{tip}}$ during the polarization reversal inside the domain volume $\Omega$.

By minimizing the free energy numerically, critical bias voltage ($V_{cr}$) was evaluated and the domain lengths were calculated at and above critical voltage using the following materials parameters[35] $P_s \approx 0.11\,\text{C/m}^2$, $\varepsilon_x \approx 5$, $\varepsilon_z = \varepsilon_y \approx 18$, $\gamma = 0.001\,\text{J/m}^2$. In our calculations, we considered the tip radius $r_{tip} = 30\,\text{nm}$, $H = 10\,\mu\text{m}$, and $h = 1\,\text{nm}$. The critical voltage was about 25 V for glycine while PFM scanning indicates domain appearance after the application of much higher voltage (~65 V). This discrepancy is might be due to instability of domains appearing under the lower voltages and their backswitching after the field removal.[19] Figure 8 compares the experimental and calculated domain lengths as a function of the voltage applied to the tip. The experimental values at low voltages deviate from the expected theoretical behavior and domain sizes are smaller than predicted ones. However, at high voltages, the experimental domain lengths are very close to those predicted by the thermodynamic theory.[26]

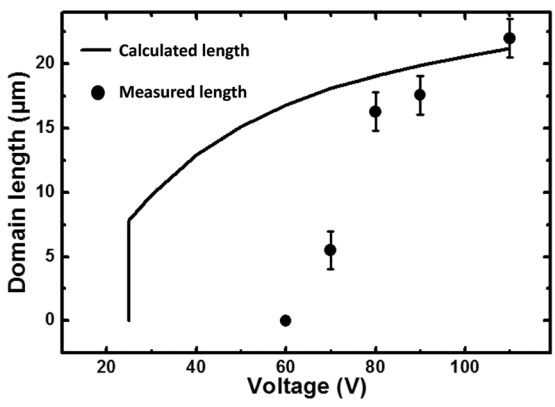


FIG. 8. Measured (filled circles) and calculated (full line) domain length in $\beta$ glycine as a function of applied voltage.

## IV. CONCLUSIONS

Our experiments have shown that solution grown microcrystals of $\beta$-glycine are uniaxial ferroelectrics with the polarization vector parallel to monoclinic axis $b$. The domain structure of $\beta$-glycine consists of charged and neutral 180° domain walls. Dynamics of these in-plane domains is studied as a function of applied voltage and pulse duration. The domain shape is dictated by the polarization screening and mediated by growth defects such as atomic steps and pits. Thermodynamic theory is applied to explain the domain propagation induced by the AFM tip. Our findings suggest that the properties of $\beta$-glycine are controlled by the charged domain walls which in turn can be manipulated by the external bias.

## ACKNOWLEDGMENTS

The work was funded by the European Commission within the FP7 Marie Curie Initial Training Network "Nanomotion" (Grant Agreement No. 290158). The work was partly supported by the Ministry of Education and Science of Russian Federation Grant No. 14.Z50.31.0034, p-220. This work was developed in the scope of the project CICECO-Aveiro Institute of Materials (Ref. FCT UID/CTM/50011/2013), financed by national funds through the FCT/MEC and when applicable cofinanced by FEDER under the PT2020 Partnership Agreement. The equipment of the Ural Center of Shared Use "Modern nanotechnology" UrFU was used.

[1]M. E. Lines and A. M. Glass, *Principles and Applications of Ferroelectrics and Related Materials* (Clarendon Press, Oxford, 1977).
[2]S. Horiuchi and Y. Tokura, Nat. Mater. **7**, 357 (2008).
[3]J. Y. Li, Y. M. Liu, Y. H. Zhang, H. L. Cai, and R. G. Xiong, Phys. Chem. Chem. Phys. **15**, 20786 (2013).
[4]S. Horiuchi, Y. Tokunaga, G. Giovannetti, S. Picozzi, H. Itoh, R. Shimano, R. Kumai, and Y. Tokura, Nature **463**, 789 (2010).
[5]D. W. Fu, W. Zhang, H. L. Cai, J. Z. Ge, Y. Zhang, and R. G. Xiong, Adv. Mater. **23**, 5658 (2011).
[6]D. W. Fu, H. L. Cai, Y. Liu, Q. Ye, W. Zhang, Y. Zhang, X. Y. Chen, G. Giovannetti, M. Capone, J. Li, and R. G. Xiong, Science **339**, 425 (2013).
[7]D. V. Isakov, E. de Matos Gomes, B. Almeida, A. L. Kholkin, P. Zelenovskiy, M. Neradovskiy, and V. Ya. Shur, Appl. Phys. Lett. **104**, 032907 (2014).
[8]V. S. Bystrov, E. Seyedhosseini, S. Kopyl, I. K. Bdikin, and A. L. Kholkin, J. Appl. Phys. **116**, 066803 (2014).

[9]A. Heredia, V. Meunier, I. K. Bdikin, J. Gracio, N. Balke, S. Jesse, A. Tselev, P. K. Agarwal, B. G. Sumpter, S. V. Kalinin, and A. L. Kholkin, Adv. Funct. Mater. **22**, 2996 (2012).
[10]E. Seyedhosseini, M. Ivanov, V. Bystrov, I. Bdikin, P. Zelenovskiy, V. Ya. Shur, A. Kudryavtsev, E. D. Mishina, A. S. Sigov, and A. L. Kholkin, Cryst. Growth Des. **14**, 2831 (2014).
[11]D. Isakov, D. Petukhova, S. Vasilev, A. Nuraeva, T. Khazamov, E. Seyedhosseini, P. Zelenovskiy, V. Shur, and A. Kholkin, Cryst. Growth Des. **14**, 4138 (2014).
[12]*Scanning Probe Microscopy: Electrical and Electromechanical Phenomena at the Nanoscale*, edited by S. Kalinin and A. Gruverman (Springer, New York, 2006), Vol. I.
[13]N. Balke, I. Bdikin, S. V. Kalinin, and A. L. Kholkin, J. Am. Ceram. Soc. **92**, 1629 (2009).
[14]S. Lei, E. A. Eliseev, A. N. Morozovska, R. C. Haislmaier, T. T. A. Lummen, W. Cao, S. V. Kalinin, and V. Gopalan, Phys. Rev. B **86**, 134115 (2012).
[15]F. Peter, B. Reichenberg, A. Rudiger, R. Waser, and K. Szot, IEEE Trans. Ultrason. Ferroelectr. Freq. Control **53**, 2253 (2006).
[16]R. E. Newnham, *Properties of Materials: Anisotropy, Symmetry, Structure* (Oxford University Press, 2005).
[17]U. Ozgur, Ya. I. Alivov, C. Liu, A. Teke, M. A. Reshchikov, S. Doğan, V. Avrutin, S. J. Cho, and H. Morkoç, J. Appl. Phys. **98**, 041301 (2005).
[18]F. Kagawa, S. Horiuchi, N. Minami, S. Ishibashi, K. Kobayashi, R. Kumai, Y. Murakami, and Y. Tokura, Nano Lett. **14**, 239 (2014).
[19]A. K. Tagantsev, L. E. Cross, and J. Fousek, *Domains in Ferroic Crystals and Thin Films* (Springer, New york, 2010).
[20]E. G. Fesenko, V. G. Gavrilyachenko, M. A. Martinenko, A. F. Semenchov, and I. P. Lapin, Ferroelectrics **6**, 61 (1973).
[21]C. L. Jea, S. B. Mi, K. Urban, I. Vrejoiu, M. Alexe, and D. Hesse, Nat. Mater. **7**, 57 (2008).
[22]E. A. Eliseev, A. N. Morozovska, G. S. Svechnikov, V. Gopalan, and V. Ya. Shur, Phys. Rev. B **83**, 235313 (2011).
[23]N. A. Pertsev, R. V. Gainutdinov, Ya. V. Bodnarchuk, and T. R. Volk, J. Appl. Phys. **117**, 034101 (2015).
[24]P. Paruch, T. Tybell, and J. M. Triscone, Appl. Phys. Lett. **79**, 530 (2001).
[25]N. A. Pertsev, A. Petraru, H. Kohlstedt, R. Waser, I. K. Bdikin, D. Kiselev, and A. L. Kholkin, Nanotechnology **19**, 375703 (2008).
[26]N. A. Pertsev and A. L. Kholkin, Phys. Rev. B **88**, 174109 (2013).
[27]A. V. Ievlev, D. O. Alikin, A. N. Morozovska, O. V. Varenyuk, E. A. Eliseev, A. L. Kholkin, V. Ya. Shur, and S. V. Kalinin, ACS Nano **9**, 769 (2015).
[28]V. V. Shur, A. R. Akhmathanov, M. A. Chuvakova, and I. S. Baturin, Appl. Phys. Lett. **105**, 152905 (2014).
[29]K. Kobayashi, S. Horiuchi, R. Kumai, F. Kagawa, Y. Murakami, and Y. Tokura, Phys. Rev. Lett. **108**, 237601 (2012).
[30]S. Horiuchi, R. Kumai, and Y. Tokura, Adv. Mater. **23**, 2098 (2011).
[31]S. Horiuchi, F. Kagawa, K. Hatahara, K. Kobayashi, R. Kumai, Y. Murakami, and Y. Tokura, Nat. Commun. **3**, 1308 (2012).
[32]M. Molotskii, A. Agronin, P. Urenski, M. Shvebelman, G. Rosenman, and Y. Rosenwaks, Phys. Rev. Lett. **90**, 107601 (2003).
[33]Y. Y. Liu, R. K. Vasudevan, K. Pan, S. H. Xie, W. I. Liang, A. Kumar, S. Jesse, Y. C. Chen, Y. H. Chu, V. Nagarajan, S. V. Kalinine, and J. Y. Li, Nanoscale **4**, 3175 (2012).
[34]T. R. Volk, R. V. Gainutdinov, Ya. V. Bodnarchuk, and L. I. Ivlev, JETP Lett. **97**, 483 (2013).
[35]V. S. Bystrov, E. Seyedhosseini, I. Bdikin, S. Kopyl, S. M. Neumayer, J. Coutinho, and A. L. Kholkin, Ferroelectrics **475**, 107 (2015).